Effect of lateral structure parameters of SiGe HBTs on synthesized active inductors*

Yan-Xiao Zhao(赵彦晓), Wan-Rong Zhang(张万荣)†, Xin Huang(黄鑫), Hong-Yun Xie(谢红云), Dong-Yue Jin(金冬月), and Qiang Fu(付强)

School of Electronic Information and Control Engineering, Beijing University of Technology, Beijing 100124, *China*

(Received 10 October 2015; revised manuscript received 8 November 2015; published online 20 January 2016)

The effect of lateral structure parameters of transistors including emitter width, emitter length, and emitter stripe number on the performance parameters of the active inductor (AI), such as the effective inductance L_s, quality factor Q, and self-resonant frequency ω_0 is analyzed based on 0.35-μm SiGe BiCMOS process. The simulation results show that for AI operated under fixed current density J_C, the HBT lateral structure parameters have significant effect on L_s but little influence on Q and ω_0, and the larger L_s can be realized by the narrow, short emitter stripe and few emitter stripes of SiGe HBTs. On the other hand, for AI with fixed HBT size, smaller J_C is beneficial for AI to obtain larger L_s, but with a cost of smaller Q and ω_0. In addition, under the fixed collector current I_C, the larger the size of HBT is, the larger L_s becomes, but the smaller Q and ω_0 become. The obtained results provide a reference for selecting geometry of transistors and operational condition in the design of active inductors.

Keywords: SiGe HBT, lateral structure parameters, active inductor

PACS: 85.30.−z, 85.30.Pq, 85.40.Qx, 84.37.+q **DOI:** 10.1088/1674-1056/25/3/038501

1. Introduction

Active inductors (AIs) synthesized by transistors have attracted increasing interest due to a number of unique advantages over its spiral counterpart including small chip area consumption, large inductance with wide tuning range, large and tunable quality factor, and high self-resonant frequency.[1–5] The popular synthesis method of AI is based on Gyrator-C principle. A gyrator consists of two back-to-back connected transistors as transconductors, and input capacitance C_π of one transconductor acts as the load of the other transconductor,[1,6] then the gyrator-C behaves as a single-ended inductor. Therefore, the performance of transistors has a decisive effect on the performance of active inductor. Furthermore, the performance of transistors is almost determined by vertical and lateral structure parameters. For the transistors with the fixed vertical structure, their performance parameters are fundamentally determined by lateral structure.[7,8] Therefore, for an AI designer who relies on the library of foundry, it is important to know how to select transistors in the foundry library so as to meet the requirement of AI parameters, such as inductance L_s, quality factor Q, and self-resonant frequency ω_0.

Up to now, there are many papers on synthesis of AI. It is shown that the AI parameters depend on the model parameters of transistors, such as capacitance, transconductance and resistance. Kia *et al.*[1,6,9] proposed novel AIs and derived that L_s can be expressed by transistor model parameters, so can Q and ω_0. Kumari *et al.*[3] studied the dependence of L_s on the load capacitance C. Robert *et al.*[10] discussed the Q enhancement with the feedback resistance R_f. Chun *et al.*[11] discussed the effect of the input signal voltage on L_s and improved the AI linearity. However, there has been no report on the effect of lateral parameters of transistors on performance parameters of AI.

In this paper, based on library of 0.35-μm SiGe BiCMOS process, the effect of lateral parameters of transistor such as emitter width, emitter length, and emitter stripe number on performance parameters of AI is investigated. The paper is arranged as follows. In Section 2, taking a typical active inductor topology for example, the dependence of the AI parameters including the L_s, Q, and ω_0 on transistor model parameters input capacitance C_π, transconductance g_m, and input resistance r_π is given. Furthermore, in Section 3, by analyzing the dependence of the transistor model parameters on HBTs lateral parameters, we obtain the analytical expressions that reveal the effect of transistor lateral parameters on the AI parameters L_s, Q, and ω_0. In Section 4, based on library of 0.35-μm SiGe BiCMOS process, the effect of lateral parameters of transistors such as emitter width, emitter length, and emitter stripe number on AI parameters is verified. Finally, the conclusion is given in Section 5.

2. A typical SiGe HBT active inductor

A typical SiGe HBT active inductor consists of common emitter configuration of transistor Q_1 with a negative transconductance and common collector configuration of transistor Q_2

*Project supported by the Natural Science Foundation of Beijing, China (Grant Nos. 4142007 and 4122014), the National Natural Science Foundation of China (Grant No. 61574010), and the Higher Educational Science and Technology Program of Shandong Province, China (Grant No. J13LN09).

†Corresponding author. E-mail: wrzhang@bjut.edu.cn

© 2016 Chinese Physical Society and IOP Publishing Ltd

with a positive transconductance, as shown in Fig. 1. The small signal equivalent circuit of the active inductor including SiGe HBT input capacitance C_π, input resistance r_π, transconductance g_m is shown in Fig. 2, and the input admittance of the active inductor Y_in can be expressed as follows:

$$Y_\mathrm{in} = \left(\frac{1}{r_{\pi 1}} + g_{\mathrm{m}1}\right) + sC_{\pi 1} + \frac{g_{\mathrm{m}1}g_{\mathrm{m}2}}{1/r_{\pi 2} + sC_{\pi 2}}. \tag{1}$$

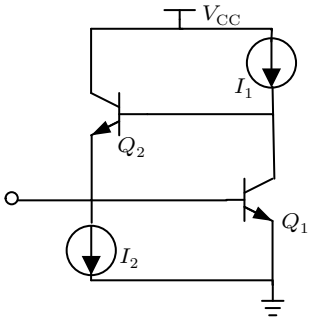


Fig. 1. A typical SiGe HBT active inductor.

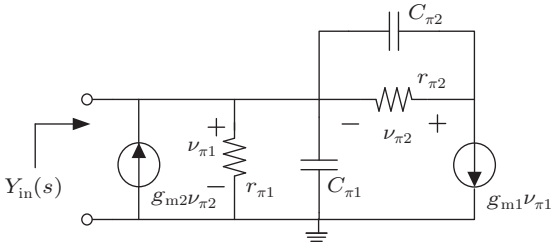


Fig. 2. Small signal equivalent circuit.

The expression (1) can be represented by an RLC network as shown in Fig. 3 with its parameters given by

$$R_\mathrm{p} = \frac{1}{1/r_{\pi 1} + g_{\mathrm{m}1}}, \tag{2}$$

$$C_\mathrm{p} = C_{\pi 1}, \tag{3}$$

$$L_\mathrm{s} = \frac{C_{\pi 2}}{g_{\mathrm{m}1}g_{\mathrm{m}2}}, \tag{4}$$

$$R_\mathrm{sL} = \frac{1}{r_{\pi 2}g_{\mathrm{m}1}g_{\mathrm{m}2}}. \tag{5}$$

The self-resonant frequency ω_0 of RLC network of the active inductor is derived from Eqs. (3) and (4) as

$$\omega_0 = \sqrt{\frac{1}{L_\mathrm{s}C_\mathrm{p}}} = \sqrt{\frac{g_{\mathrm{m}1}}{C_{\pi 1}}\frac{g_{\mathrm{m}2}}{C_{\pi 2}}}. \tag{6}$$

The input impedance $Z_\mathrm{in} = 1/Y_\mathrm{in}$ has a zero at frequency

$$\omega_\mathrm{z} = \frac{1}{C_{\pi 2}r_{\pi 2}}. \tag{7}$$

It is evident that the RLC network in Fig. 3 is inductive when $\omega_\mathrm{z} < \omega < \omega_0$.

The quality factor Q of the active inductor can be expressed as

$$Q = \frac{R_\mathrm{p}//R_\mathrm{pL}}{\omega L_\mathrm{s}} = \frac{r_{\pi 1}r_{\pi 2}g_{\mathrm{m}1}g_{\mathrm{m}2}}{\omega(r_{\pi 2}C_{\pi 2} + g_{\mathrm{m}1}r_{\pi 1}r_{\pi 2}C_{\pi 2} + r_{\pi 1}C_{\pi 1})}, \tag{8}$$

where "//" represents R_p in parallel with R_pL, and $R_\mathrm{pL} \approx L_\mathrm{s}/(R_\mathrm{sL}C_\mathrm{p})$.[12]

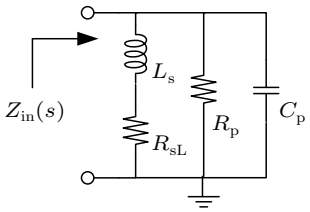


Fig. 3. RLC equivalent circuit.

3. Analytical expressions for AI parameters dependence on lateral structure parameters of SiGe HBTs

As shown in Section 2, the active inductor parameters L_s, Q, and ω_0 depend on transistor model parameters C_π, g_m, and r_π. Obviously, they depend on the lateral structure parameters of the transistors. Therefore, the effect of the lateral structure parameters of SiGe HBTs on the AI is obtained by analyzing the dependence of C_π, g_m, and r_π on lateral structure parameters.

In general, the input resistance r_π of the transistor is expressed as

$$r_\pi = \frac{\beta_0}{g_\mathrm{m}}, \tag{9}$$

where β_0 is the small-signal current gain of the transistor, and β_0 can be calculated by

$$\beta_0 = \left(\frac{W_\mathrm{B}^2}{2\tau_\mathrm{n}D_\mathrm{n}} + \frac{D_\mathrm{p}}{D_\mathrm{n}}\frac{W_\mathrm{B}}{L_\mathrm{p}}\frac{N_\mathrm{A}}{N_\mathrm{D}}\right)^{-1}, \tag{10}$$

where W_B is the width of the base, τ_n is the minority-carrier lifetime in the base, D_n is the diffusion coefficient for electrons, D_p is the diffusion coefficient for holes, L_p is the diffusion length for holes in the emitter, N_A is doping density of the base, N_D is doping density of the emitter. Equation (10) indicates that β_0 is related mainly to the vertical structure parameters, and it is almost independent of the lateral structure parameters.

The transconductance g_m of the transistor can be expressed as

$$g_\mathrm{m} = \frac{qI_\mathrm{C}}{kT} = \frac{qJ_\mathrm{C}W_\mathrm{E}L_\mathrm{E}N_\mathrm{E}}{kT}, \tag{11}$$

where I_C is the current of collector, J_C is the current density of collector, q is the electron charge, k is the Boltzmann's constant, T is the temperature, W_E is the emitter width, L_E is the emitter length, and N_E is the emitter stripe number.

The input capacitance C_π is composed of a bottom capacitance ($C_{\rm Bottom}$) and a sidewall capacitance ($C_{\rm SW}$), and C_π can be simply described as

$$C_\pi \cong AW_{\rm E}L_{\rm E}N_{\rm E} + 2B(W_{\rm E}+L_{\rm E})D_{\rm E}N_{\rm E}, \tag{12}$$

where A and B are respectively capacitance per unit area for the bottom part and sidewall part, and $D_{\rm E}$ is the junction depth of emitter. Because $D_{\rm E}$ in the library of 0.35 μm SiGe BiCMOS technology is fixed, the capacitance is then proportional to $W_{\rm E}$, $L_{\rm E}$, and $N_{\rm E}$. Generally, $L_{\rm E}$ is much greater than $W_{\rm E}$, and it can be considered that $W_{\rm E}+L_{\rm E}\approx L_{\rm E}$, and equation (13) can be simplified as

$$C_\pi \cong AW_{\rm E}L_{\rm E}N_{\rm E} + 2BL_{\rm E}D_{\rm E}N_{\rm E}. \tag{13}$$

For simplification, the transistors Q_1 and Q_2 in Fig. 1 is assumed to be identical. Therefore, they have the same r_π, C_π, and $g_{\rm m}$. The inductance $L_{\rm s}$ can be derived by substituting Eqs. (11) and (13) into Eq. (4)

$$\begin{aligned} L_{\rm s} &= \frac{C_\pi}{g_{\rm m}g_{\rm m}} \\ &= \frac{k^2T^2}{q^2I_{\rm C}^2}\left(AW_{\rm E}L_{\rm E}N_{\rm E}+2BL_{\rm E}D_{\rm E}N_{\rm E}\right) \\ &= \frac{k^2T^2}{q^2J_{\rm C}^2W_{\rm E}L_{\rm E}N_{\rm E}}\left[A+\frac{2BD_{\rm E}}{W_{\rm E}}\right]. \end{aligned} \tag{14}$$

As shown in Eq. (14), the inductance is larger for smaller size of SiGe HBT at fixed $J_{\rm C}$, and inversely at fixed $I_{\rm C}$.

Quality factor Q is derived by substituting Eqs. (9), (11), and (13) into Eq. (8)

$$\begin{aligned} Q &= \omega\left(\frac{2C_\pi}{r_\pi g_{\rm m}g_{\rm m}}+\frac{C_\pi}{g_{\rm m}}\right)^{-1} \\ &= \left[\omega\left(\frac{2}{\beta_0}+1\right)\frac{kT}{qJ_{\rm C}}\left(A+\frac{2BD_{\rm E}}{W_{\rm E}}\right)\right]^{-1}. \end{aligned} \tag{15}$$

Because $\beta_0 \gg 1$, $(2/\beta_0+1)\approx 1$, equation (15) is simplified into

$$\begin{aligned} Q &= \frac{qI_{\rm C}}{\omega kT\left(AW_{\rm E}L_{\rm E}N_{\rm E}+2BL_{\rm E}D_{\rm E}N_{\rm E}\right)} \\ &= \left[\omega\frac{kT}{qJ_{\rm C}}\left(A+\frac{2BD_{\rm E}}{W_{\rm E}}\right)\right]^{-1}. \end{aligned} \tag{16}$$

Equation (16) implies that Q is independence of $L_{\rm E}$ and $N_{\rm E}$, and Q is larger with wider $W_{\rm E}$ at fixed $J_{\rm C}$. On the other hand, Q is lower with larger size of SiGe HBT at fixed $I_{\rm C}$. In addition, Q is inversely proportional to the angular frequency ω and proportional to collector current density $J_{\rm C}$.

The quality factor Q is also expressed as follows:

$$Q=\left[\omega\left(\frac{2C_\pi}{r_\pi g_{\rm m}g_{\rm m}}+\frac{C_\pi}{g_{\rm m}}\right)\right]^{-1}\approx\left[\omega\frac{C_\pi}{g_{\rm m}}\left(\frac{2}{\beta_0}+1\right)\right]^{-1}\approx\frac{\omega_0}{\omega}. \tag{17}$$

Therefore, ω_0 can be given by

$$\omega_0 = \omega Q. \tag{18}$$

4. Verification and discussion

4.1. Effect of emitter width on performance parameters of the active inductor

Figure 4 shows the equivalent inductance $L_{\rm s}$ versus $1/W_{\rm E}$ at different frequency of 2 GHz, 6 GHz, and 7 GHz, respectively, for SiGe HBTs with $L_{\rm E}=10$ μm and $N_{\rm E}=1$ at a fixed $J_{\rm C}=0.05$ mA/μm^2. As $W_{\rm E}$ increases from 0.3 μm to 0.9 μm, a decrease of 3.2 nH at $f=2$ GHz and $f=6$ GHz, and a 2.7 nH decrease at $f=7$ GHz is observed. It indicates that $L_{\rm s}$ increases as $W_{\rm E}$ decreases for a given frequency. Therefore, a large $L_{\rm s}$ can be obtained by small $W_{\rm E}$, which is consistent with Eq. (14).

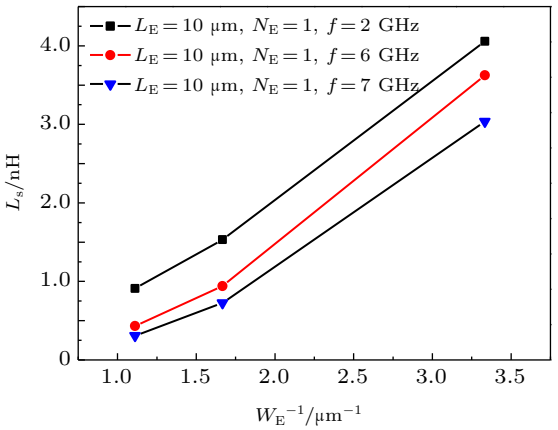


Fig. 4. (color online) $L_{\rm s}$ versus $1/W_{\rm E}$ at $J_{\rm C}=0.05$ mA/μm^2.

Figure 5 gives Q and ω_0 of the AI versus $W_{\rm E}$ at a fixed $J_{\rm C}=0.05$ mA/μm^2. As $W_{\rm E}$ increases from 0.3 μm to 0.9 μm, Q has an increase of 0.5 at $f=2$ GHz and an increase of 0.3 at $f=6$ GHz and $f=7$ GHz, and ω_0 has an increase of 1 GHz. It is shown that Q and ω_0 increase slightly with increasing $W_{\rm E}$, which is consistent with Eqs. (16) and (18).

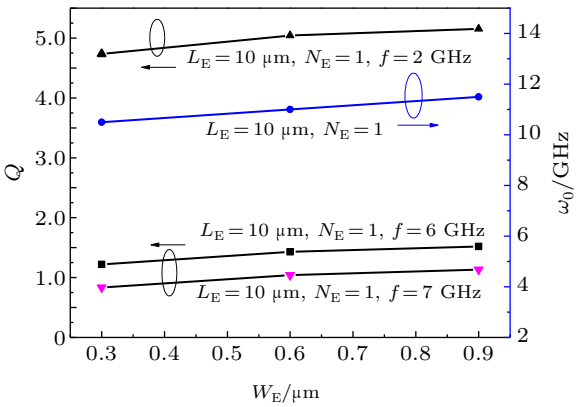


Fig. 5. (color online) Q and ω_0 versus $W_{\rm E}$ at $J_{\rm C}=0.05$ mA/μm^2.

Figure 6 shows $L_{\rm s}$, Q, and ω_0 of the AI versus $W_{\rm E}$ for SiGe HBTs with $L_{\rm E}=15$ μm and $N_{\rm E}=1$ at $I_{\rm C}=0.2$ mA and $f=1$ GHz. As $W_{\rm E}$ increases from 0.3 μm to 0.9 μm, $L_{\rm s}$ has an increase of 2.79 nH, Q has a decrease of 1.07 and ω_0 has

a decrease of 4.5 GHz. It indicates that L_s increases with W_E because L_s is proportional to C_π and inversely proportional to the square of g_m. As we know, wider W_E leads to larger C_π, and g_m is independence of W_E at fixed collector current I_C. Inversely, wider W_E results in smaller Q because Q is inversely proportional to C_π at fixed collector current I_C. Similarly to Q, ω_0 decreases with the increase of W_E.

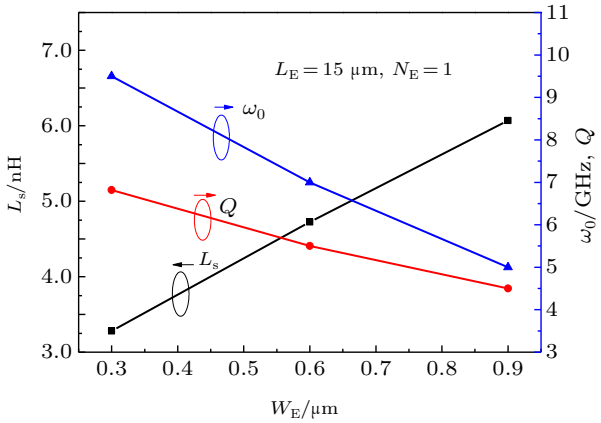


Fig. 6. (color online) L_s, Q, and ω_0 versus W_E at $I_C = 0.2$ mA.

4.2. Effect of emitter length on performance of the active inductor

Figure 7 shows the equivalent inductance L_s versus $1/L_E$ at different frequency of 2 GHz, 6 GHz, and 7 GHz, respectively, for SiGe HBTs with $W_E = 0.3$ μm and $N_E = 1$ at a fixed $J_C = 0.05$ mA/μm^2. As emitter length increases from 10 μm to 20 μm, L_s is reduced by 2.1 nH at f=2 GHz, 1.8 nH at $f = 6$ GHz, and 1.4 nH at $f = 7$ GHz. Therefore, larger L_s can be obtained by narrowing down L_E, which is consistent with Eq. (14).

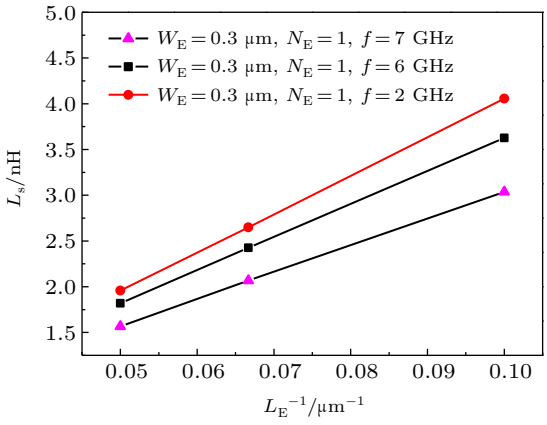


Fig. 7. (color online) L_s versus $1/L_E$ at $J_C = 0.05$ mA/μm^2.

Figure 8 gives Q and ω_0 of the active inductor versus $1/L_E$ at $J_C = 0.05$ mA/μm^2. As emitter length increases from 10 μm to 20 μm, Q is reduced by 0.19 at $f = 2$ GHz, 0.1 at $f = 6$ GHz, and 0.08 at $f = 7$ GHz, and ω_0 is 10.5 GHz as emitter length is 10 μm, 15 μm, and 20 μm. It illustrates that L_E has little effect on Q and ω_0, which is consistent with Eqs. (16) and (18).

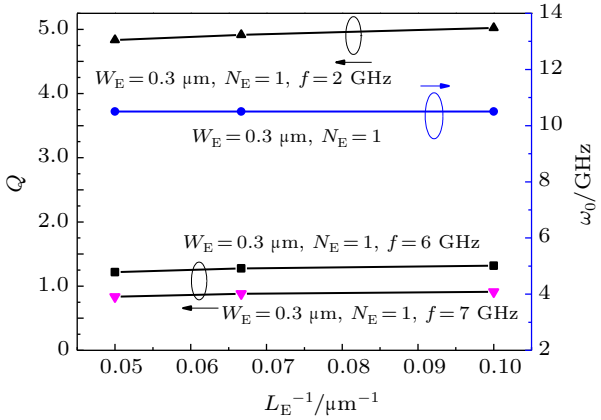


Fig. 8. (color online) Q and ω_0 versus $1/L_E$ at $J_C = 0.05$ mA/μm^2.

Figure 9 shows L_s, Q, and ω_0 of the active inductor versus L_E for SiGe HBTs with $W_E = 0.3$ μm and $N_E = 1$ at $I_C = 0.2$ mA and $f = 1$ GHz. As L_E increases from 10 μm to 20 μm, L_s has an increase of 1.61 nH, but Q is reduced by 2.66 and ω_0 is lowered from 13.5 GHz to 7 GHz. It indicates that under fixed collect current I_C, larger L_s can be obtained by longer emitter length, but this can lower Q and ω_0.

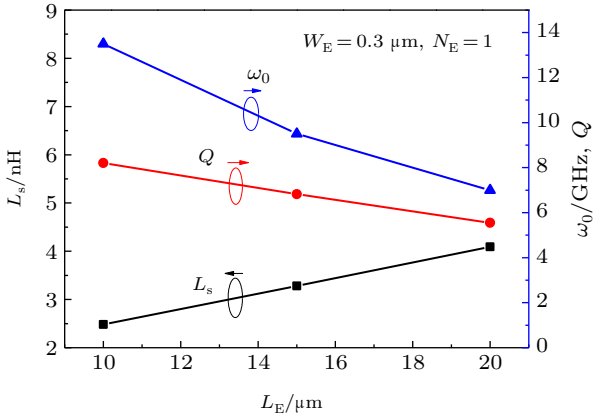


Fig. 9. (color online) L_s, Q, and ω_0 versus L_E at $I_C = 0.2$ mA.

4.3. Effect of emitter stripe number on performance of the active inductor

Figure 10 shows the equivalent inductance L_s versus $1/N_E$ at different frequency of $f = 2$ GHz, 6 GHz, and 7 GHz, respectively, for SiGe HBTs with $W_E = 0.3$ μm and $L_E = 10$ μm at a fixed $J_C = 0.05$ mA/μm^2. As emitter stripe number increases from 1 to 5, L_s is reduced by 3.25 nH at $f = 2$ GHz, 2.89 nH at $f = 6$ GHz, and 2.43 nH at $f = 7$ GHz. Therefore, larger L_s can be obtained by smaller N_E, which is consistent with Eq. (14).

Figure 11 gives Q and ω_0 of the active inductor versus $1/N_E$ at $J_C = 0.05$ mA/μm^2. As emitter stripe number increases from 1 to 5, Q is reduced by 0.1 at $f = 2$ GHz, 6 GHz, and 7 GHz, and ω_0 is 10.5 GHz as emitter stripe number is 1,

3, and 5. It illustrates that N_E has little effect on Q and ω_0, which is consistent with Eqs. (16) and (18).

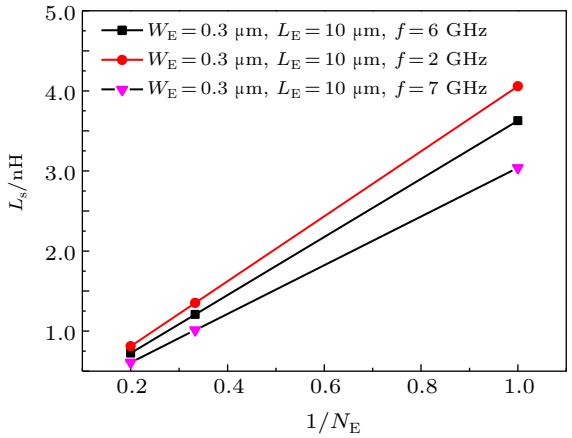


Fig. 10. (color online) L_s versus $1/L_E$ at $J_C = 0.05$ mA/μm^2.

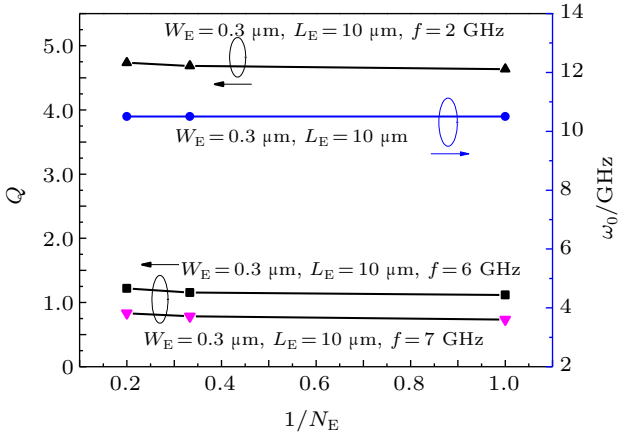


Fig. 11. (color online) Q and ω_0 versus $1/N_E$ at $J_C = 0.05$ mA/μm^2.

Figure 12 shows L_s, Q, and ω_0 of the active inductor versus N_E for SiGe HBTs with $W_E = 0.3$ μm and $L_E = 10$ μm at a fixed $I_C = 0.2$ mA and $f = 1$ GHz. As N_E increases from 1 to 5, L_s increases from 2.48 nH to 8.89 nH, Q decreases from 8.21 to 2.06, ω_0 reduces from 13.5 GHz to 2.5 GHz. It can be seen that L_s becomes larger, but Q and ω_0 become lower with more emitter stripes in parallel.

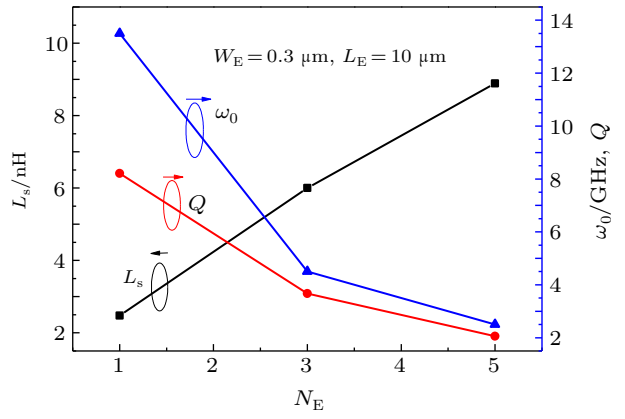


Fig. 12. (color online) L_s, Q, and ω_0 versus W_E at $I_C = 0.2$ mA.

4.4. Effect of collect current density on performance of the active inductor

The above results are obtained at the fixed collect current density and the fixed collect current, respectively. Figure 13 shows the active inductor parameters L_s, Q, and ω_0 versus the collect current density J_C for SiGe HBTs with $W_E = 0.3$ μm, $L_E = 10$ μm, and $N_E = 1$ at $f = 2.5$ GHz. As collect current density increases from 0.02 to 0.20 mA/μm^2, L_s reduces from 16.1 nH to 0.44 nH, Q increases from 0.95 to 19.10, and ω_0 increases from 4 GHz to 33.5 GHz. It indicates that smaller J_C is beneficial for active inductor to obtain larger L_s, but higher Q and ω_0 need active inductor operates at larger J_C.

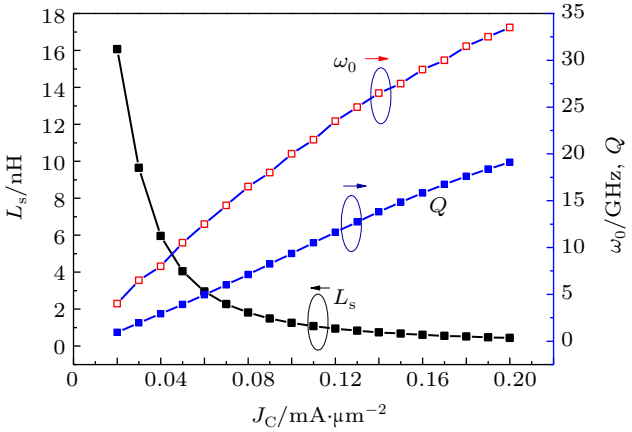


Fig. 13. (color online) L_s, Q, and ω_0 versus the collect current density J_C at a fixed size of HBTs.

5. Conclusion

In the paper, we analyze the effect of lateral structure parameters including emitter width, length and emitter stripe number of HBT on the performance parameters of the active inductor (AI), such as inductance L_s, quality factor Q, and self-resonant frequency ω_0 based on library of 0.35-μm SiGe BiCMOS process. The simulation results show that for a given collector current density J_C, the large L_s of the AI can be obtained by the narrow, short emitter stripe and few emitter stripes, but Q and ω_0 have little dependence on the geometry sizes of SiGe HBTs. For a fixed HBT size, smaller J_C is beneficial for AI to obtain larger L_s, but with a cost of smaller Q and ω_0. In addition, for the fixed collector current I_C, the large HBT size results in large L_s, but small Q and ω_0. Therefore, in the design of an AI, a tradeoff exists among the AI parameters, the lateral structure parameters of HBT, and operational current density or operational current. The obtained results provide a basis for selecting the transistors lateral geometry from the library of foundry and operational condition in the design of active inductors.

References

[1] Kia H B 2014 22*nd Iranian Conference on Electrical Engineering*, May 20–22, 2014, Tehran, p. 1

[2] RejaM M, Moez K and Filanovosky I 2010 *IEEE Transactions on Circuits and Systems: Express Briefs.* **57** 587

[3] KumariK S and Bhuvan B 2011 *International Conference on Devices and Communications*, February 24–25, 2011, Mesra, India, p. 1

[4] Zito D, Pepe D and Fonte A 2012 *IEEE Microwave and Wireless Components Letters* **22** 138

[5] Zhang S J, Zhang X X and Liu Y 2012 *Chin. Phys. Lett.* **29** 084217

[6] Selvathi D and Pown M 2014 *International Conference on Communication and Network Technologies*, December 18–19, 2014, Sivakasi, p. 296

[7] Fu Q, Zhang W R, Jin D Y, Ding C B, Zhao Y X and Lu D 2014 *Chin. Phys. B* **23** 114402

[8] Lin C H, Su Y K, Juang Y Z, Chuang R W, Chang S J, Chen J F and Tu C H 2004 *IEEE Transactions on Microwave Theory and Techniques* **52** 2153

[9] Chao C H, Chin W K, Chien C H and Yi J C J 2002 *IEEE Microwave and Wireless Components Letters* **12** 467

[10] Robert F, Cathelin P, Diet A and Villegas M 2011 *IEEE 12th Annual Wireless and Microwave Technology Conference* (*WAMICON*), April 18–19, 2011, Clearwater Beach, FL, p. 1

[11] Chun L L, A'ainA K B and Kordesch A V 2009 *IEEE Transactions on Microwave Theory and Techniques* **57** 1915

[12] Clarke K K and HessD T 1978 *Communication Circuits: Analysis and Design*, 2nd edn. (Addison-Wesley Publishing Company) p. 358